

RESEARCH ARTICLE

Open Access



MyD88 inhibitor TJ-M2010-5 alleviates spleen impairment and inflammation by inhibiting the PI3K/miR-136-5p/AKT3 pathway in the early infection of *Trichinella spiralis*

Huifang Bai^{1†}, Qianqian Dang^{1†}, Guoliang Chen^{1†}, Lingfeng Xie¹, Saining Wang¹, Ning Jiang¹, Xiaoxia Wu¹, Shuyan Zhang¹ and Xuelin Wang^{1*} 

Abstract

Trichinella spiralis (*T. spiralis*) has been reported to induce inflammation, which can cause immune system dysregulation. Myeloid differentiation primary response gene 88 (MyD88) is implicated in inflammation signalling pathways. TJ-M2010-5 is a novel MyD88 inhibitor with remarkable protective effects against several diseases. However, the precise mechanism of TJ-M2010-5's involvement in spleen impairment and inflammation in the early infection of *T. spiralis* has yet to be fully elucidated. This study analysed histological, inflammation, and macrophage polarisation of the early *T. spiralis*-infected mice treated with TJ-M2010-5. MyD88 promoter methylation results showed that the methylation levels in the 5 d group were lower compared to the control group ($P < 0.05$). Furthermore, the methylation led to an imbalance in anti-inflammatory regulation in the infected mice. After TJ-M2010-5 treatment, spleen impairment was reduced. Sequencing analysis showed that TJ-M2010-5 significantly up-regulated 9 and down-regulated 10 miRNAs compared with the 5 d group. A dual-luciferase reporter assay further revealed that miR-136-5p is involved in the TJ-M2010-5 treatment by targeting AKT3. In RAW264.7 cells, TJ-M2010-5 pre-treatment significantly reversed the M1 polarisation and inhibited nitric oxide (NO) production. LC-MS/MS results showed TJ-M2010-5 was hepatosplenic-targeted. In conclusion, the study demonstrates that TJ-M2010-5 could effectively alleviate spleen impairment and reduce inflammation in mice infected with *T. spiralis* in its early stages by blocking the activation of PI3K/miR-136-5p/AKT3.

Keywords TJ-M2010-5, MyD88, inflammation, *Trichinella spiralis*, methylation

Handling editor: Frank Katzer.

[†]Huifang Bai, Qianqian Dang and Guoliang Chen contributed equally to this work.

*Correspondence:
Xuelin Wang
xuelin@jlu.edu.cn



© The Author(s) 2025. **Open Access** This article is licensed under a Creative Commons Attribution 4.0 International License, which permits use, sharing, adaptation, distribution and reproduction in any medium or format, as long as you give appropriate credit to the original author(s) and the source, provide a link to the Creative Commons licence, and indicate if changes were made. The images or other third party material in this article are included in the article's Creative Commons licence, unless indicated otherwise in a credit line to the material. If material is not included in the article's Creative Commons licence and your intended use is not permitted by statutory regulation or exceeds the permitted use, you will need to obtain permission directly from the copyright holder. To view a copy of this licence, visit <http://creativecommons.org/licenses/by/4.0/>. The Creative Commons Public Domain Dedication waiver (<http://creativecommons.org/publicdomain/zero/1.0/>) applies to the data made available in this article, unless otherwise stated in a credit line to the data.

Introduction

Trichinella spiralis (*T. spiralis*) are foodborne zoonosis parasites and a pathogen of trichinellosis. When infected with *T. spiralis*, the host experiences chronic inflammation for a prolonged period and exhibits immune disorders [1]. The host can also experience two types of tissue damage: direct damage caused by the pathogen and immunopathological damage. The spleen is a vital peripheral immune organ comprising an abundance of immune cells, including T and B lymphocytes, monocytes, macrophages, and dendritic cells. It plays a crucial role in the onset and progression of various diseases. However, spleen impairment and its effect on immune regulation remain unknown during the early infection of *T. spiralis*.

Studies have shown that initiating immune responses in resisting pathogens is closely correlated with toll-like receptors (TLRs) [2]. As pro- or anti-inflammatory molecules and signalling molecules in the TLR pathways, they can activate the host's innate immune system to recognise various pathogens and defend against their invasion. Toll/IL-1R (TIR) is an essential cytoplasmic adaptor molecule coupled with myeloid differentiation primary response gene 88 (MyD88) [3]. MyD88 can interact with TIR domains to recognise various TLRs without TLR3.

In one study, alleviating inflammation was achieved by delaying the assembly of MyD88 and TLR4 during *T. spiralis* infection [4]. Ma et al. reported that *T. spiralis* galectin (Tsgal) binding to TLR4 in the gut epithelium activated the MAPK-NF- κ B pathway, induced the expression of TLR4 and pro-inflammatory cytokines, induced intestinal inflammation, and mediated larval invasion of the gut mucosa [5]. Furthermore, according to another study, galactomannan can bind to recombinant *T. spiralis* galectin (rTsgal), inhibiting the ability of rTsgal to facilitate larval invasion of intestinal epithelial cells (IECs) in vitro. This process was influenced by the polarisation of macrophages towards an M1 phenotype, resulting in increased antibody-dependent cytotoxicity (ADCC) against newborn larvae (NBL) [6]. Macrophages are not only rich in TLR4 receptors on their surface but also play an important role in the immune response to parasitic infections [7].

It has also been shown that rTsCatL2 (recombinant *T. spiralis* cathepsin L domains)-induced M1-type RAW264.7 results in the death of *T. spiralis* NBL [8]. Furthermore, rTsDPP1 (recombinant *T. spiralis* dipeptidyl peptidase 1) promotes macrophage polarisation towards the M2 phenotype. This promotion increases the expression of anti-inflammatory cytokines and suppresses macrophage-mediated ADCC by activating the STAT6/PPAR γ pathway. This mechanism facilitates the parasitism and immune evasion of the nematode [9]. Therefore,

it is essential to study the role of macrophages in the early infection of *T. spiralis*.

Further studies have suggested that DNA methylation and noncoding small RNAs (18~22 nucleotides) can contribute to a coordinated epigenetic control of gene expression [10]. Regulating gene expression at transcriptional and posttranscriptional levels can involve pathogen infection [11, 12]. Furthermore, microRNA (miRNA) is a vital regulator in down-regulating drug function genes [13]. Of particular interest, one study demonstrated that noncoding small RNAs, including miRNAs, can regulate the development of parasitic diseases [14]. However, the miRNA regulation mechanism was still not shown during the early infection of *T. spiralis*. As a novel MyD88 inhibitor, TJ-M2010-5 has remarkable protective effects in treating colitis, liver fibrosis, renal interstitial fibrosis, and myocardial ischaemia/reperfusion injury [15, 16]. However, the precise molecular regulatory mechanisms of TJ-M2010-5 and its regulation by miRNAs in the development of inflammatory diseases caused by early *T. spiralis* infection are poorly understood.

This study aimed to evaluate the protective role of TJ-M2010-5 on spleen impairment and inflammation in early *T. spiralis*-infected mice. To assess spleen impairment and inflammation, we examined histological changes and macrophage polarisation. Furthermore, we evaluated the methylation rate of the MyD88 promoter in spleen tissues from mice infected early with *T. spiralis*. Microarray analysis was used to explore the expression profiles of miRNAs in spleen tissue, focusing on miR-136-5p, which was considered a promising candidate for regulating inflammation in the TJ-M2010-5-treated group. In conclusion, we intended to reveal that TJ-M2010-5 up-regulated miR-136-5p levels, changing the imbalance in anti-inflammatory regulation induced by the MyD88 promoter methylation and alleviating inflammatory responses by involving the PI3K/AKT3 pathway.

Materials and methods

Animals, parasites, drugs and tissue collection

The female BALB/c mice (weight 18 ± 2 g) were purchased from the Experimental Animal Center of College of Basic Medical Sciences, Jilin University (Changchun, China). All mice were raised and handled according to the National Institutes of Health guidelines for the care and use of laboratory animals and were approved by the Ethics Committee for Animal Experiments of Jilin University (NO. 202201-104, date: 25/2/2022).

T. spiralis (ISS534 strain) muscle larvae (ML) were maintained by serial passage in ICR mice. ML was used to orally infect mice with 250 larvae each for the infection groups. TJ-M2010-5 (MedChemExpress, Princeton,

NJ, USA) was dissolved in dimethyl sulfoxide (DMSO) at 50 °C with continuous stirring for 30 min. For the protein expression of MyD88 in spleen tissues, the animals were divided as follows (three mice per group): 0 d group: non-infected mice; 3 d, 5 d, 9 d, and 20 d group: infected mice sacrificed at 3, 5, 9, 20 days post-infection (dpi), respectively.

For other animal experiments, the mice were divided into three groups (three mice per group): Group i (0 d): non-infected mice; Group ii (5 d): infected mice sacrificed at 5 dpi; Group iii (TJ5_5 d): infected mice, the first administration on the second day after infection, followed by an intraperitoneal injection TJ-M2010-5 for five successive days (30 mg/kg/day) and sacrificed at 5 dpi. Peripheral blood samples from the mice were collected to separate the sera and were stored at -80 °C. Spleen samples were also obtained for further experiments.

For tissue distribution experiments, fifteen mice were randomly divided into five groups (three mice per group). The mice in each group were sacrificed at 0.5, 2, 6, 12, and 48 h after receiving an intraperitoneal injection of TJ-M2010-5 (30 mg/kg). Subsequently, major organs were acquired: liver, spleen, lung, and kidney. Tissues were weighed, homogenised in 70% acetonitrile and stored at -80 °C to analyse.

Cell culture

The mouse macrophage cell line RAW264.7 and the human embryonic kidney 293 T cell line HEK 293 T were purchased from the Culture Collection of the Chinese Academy of Sciences (Shanghai, China). RAW264.7 cells were cultured in RPMI 1640 medium (Gibco, Grand Island, NY, USA) at 37 °C in a humidified incubator containing 5% CO₂. HEK 293 T cells were grown in DMEM/High-Glucose culture medium (Gibco, Grand Island, NY, USA) per the above process.

Histological analysis

The spleen tissue samples collected from the grouped mice were fixed with 4% paraformaldehyde. Following dehydration, these tissues were embedded in paraffin and cut into 5 µm slices to stain with haematoxylin and eosin (H&E) (Solarbio, Beijing, China). Images of the stained cells were visualised by the microscope (OLYMPUS TH4-200, Olympus, Tokyo, Japan).

Bisulfite sequencing PCR (BSP)

Genomic DNA was extracted using the EZ DNA Methylation Gold™ kit (Zymo Research, Orange, CA, USA). The NanoDrop 2000 Spectrometer (Thermo Scientific, Waltham, MA, USA) was used to detect DNA quantity and purity (A260/A280 ratio). The study intercepted the transcription start site of the 2000-bp gene upstream

of MyD88 in the promoter region of the MyD88 CpG islands (CGIs). PCR was performed using HotStar Taq polymerase (Takara, Beijing, China). PCR used the primers (Forward: 5'- GAGGGGTTTTATTTTGAAGTT TTTA -3', Reverse: 5'- CCTATTCCCTAAAACCTCA CACCCAA -3'). The primers used were designed using the online MethPrimer software. The PCR products were electrophoresed in 1% agarose gels and visualised by ultraviolet illumination.

DNMTs and TETs activity assay

Cytoplasmic and nuclear proteins from spleen tissues were extracted using a nuclear extraction kit (Solarbio, Beijing, China). According to the instructions, the enzyme activity of DNMTs (DNA methyltransferases) and TETs (ten-eleven translocation proteins) was assessed using DNMTs activity assay colourimetric kit (Epigentek, Farmingdale, NY, USA) and TETs activity assay colourimetric kit (Epigentek). The optical density (OD) values in the assay were obtained by BioTek Cytation5 with Gen5 software (Agilent, Santa Clara, CA, USA).

Macrophage M/M2 ratio analysis in spleen tissues by flow cytometry

Suspensions of single cells from the spleen tissues of the experimental mice were prepared. The cells were stained using anti-mouse F4/80 PE (BioLegend, San Diego, CA, USA), anti-mouse CD86 FITC (BioLegend) and anti-mouse CD206 APC antibodies (Invitrogen, Waltham, MA, USA) at 37 °C for 30 min. Cells were detected and analysed by FACSCalibur (BD Biosciences, San Diego, CA, USA) and FlowJo software (TreeStar, Ashland, OR, USA), respectively.

Enzyme-linked immunosorbent assay (ELISA)

The concentrations of interleukin (IL)-4, IL-13, IL-12p70, and TNF-α in serum were quantified using an ELISA kit (Proteintech Group, Chicago, IL, USA) according to the manufacturer's guidelines.

miRNA expression profiling

The differentially expressed miRNAs (DEmiRNAs) were analysed by miRNA sequencing as previously described [17, 18]. The miRNA library and deep sequencing were then constructed by Novogene Bioinformatics Technology Co., Ltd (Beijing, China) and DESeq 2 (1.14.1) was used to conduct the differential expression analysis [19]. Venn diagrams, volcano plots, and heatmaps of DEmiRNAs were drawn by the R package (version 3.5.1, New Zealand, University of Auckland). Finally, the change in the expression of the selected miRNAs was verified by

quantitative real-time PCR (qPCR). The specific primers are shown in Additional file 1.

miRNA target genes prediction and validation

We used miRDB and TargetScan7.2 to predict the target genes of miR-136-5p. The overlapping predicted genes were selected for further analysis. The AKT3 gene's wild-type (WT) or mutated-type (MUT) 3' untranslated region (UTR) was successfully inserted into the pmirGLO luciferase reporter vector (Promega, Madison, WI, USA). The recombinant plasmids were purified using the EndoFree Plasmid Maxi Kit (Vazyme, Nanjing, China). The HEK 293 T cells were co-transfected with miR-136-5p mimics or mimics negative control (NC) and AKT3 WT plasmid or AKT3 MUT plasmid using Lipo2000 transfection reagent (Promega, Madison, WI, USA). This transfection process was carried out for 24 h. For this experiment, there were four groups, including miR-136-5p mimics+AKT3 WT, mimics NC+AKT3 WT, miR-136-5p mimics+AKT3 MUT, and mimics NC+AKT3 MUT. The Dual-Glo luciferase reporter assay system (Beyotime Biotechnology, Haimen, China) was used to assay the luciferase activity after the transfection of plasmids.

Cell viability assay

TJ-M2010-5 (0, 5, 10, 20, 30, 40, 50 μ M) were pre-treated with RAW264.7 cells. The viability of the cells was determined using a CCK-8 kit (Solarbio, Beijing, China), following the manufacturer's instructions. After culturing for 24 h, a CCK-8 kit was used again to assay the cell viability and the OD value at 450 nm was measured.

Total RNA extraction and quantitative polymerase chain reaction

Total RNA from cells was extracted using TRIzol reagent (Invitrogen, Waltham, MA, USA). RNA concentrations were determined using a NanoDrop™ 2000 (Thermo Fisher Scientific, Waltham, MA, USA). According to the protocols, all reactions were conducted by ABI 7500 real-time PCR system (Applied Biosystems, Thermo Fisher Scientific, Waltham, MA, USA). The $2^{-\Delta\Delta CT}$ method was used to calculate the comparative threshold cycle (CT) value. The specific primers are shown in Additional file 1.

Nitric oxide assay

RAW264.7 cells pre-treated with TJ-M2010-5 were incubated for 6 h. The culture medium was supplemented with LPS (1 μ g/mL). After incubation for 24 h, NO production was analysed using the Griess Reagent System (Beyotime Biotechnology, Haimen, China).

Macrophage M/M2 ratio analysis in RAW264.7 cells by flow cytometry

RAW264.7 cells were stained using anti-mouse F4/80 PE (BioLegend), anti-mouse CD86 FITC (BioLegend), and anti-mouse CD206 APC antibodies (Invitrogen, Waltham, MA, USA) at 37 °C for 30 min. Cells were detected and analysed by FACSCalibur (BD Biosciences, San Diego, CA, USA) and FlowJo software (TreeStar, Ashland, OR, USA), respectively.

Western blot

Cell and tissue lysis was performed using a radioimmunoprecipitation assay (RIPA) lysis buffer (Solarbio, Beijing, China). The cytosolic and nuclear extracts were prepared as previously described. Proteins were isolated by sodium dodecyl sulfate–polyacrylamide gel electrophoresis (SDS–PAGE) and transferred onto nitrocellulose filter (NC) membranes (Millipore, Billerica, MA, USA). NC membranes were blocked with 5% skim milk for 1 h at 37 °C and sustained shaking. After washing with Tris-buffered saline and Tween 20 (TBST) thrice, NC membranes were incubated overnight with primary antibodies at 4 °C. After incubating with secondary antibodies for 1 h at 37 °C and washing, we detected the immunoreactive bands using the Millipore chemiluminescent HRP reagent. Protein bands were recorded with a UVP ChemStudio (Analytik Jena, Germany). All antibodies are listed in Additional file 2.

Liquid chromatography–tandem mass spectrometry (LC–MS/MS)

For the linearity curve generation, TJ-M2010-5 in DMSO was diluted with ddH₂O to make serial concentrations of the calibration standards solutions (50, 100, 200, 400 and 1000 ng/mL). Subsequently, 1 μ L of the supernatant from the tissue homogenates (liver, spleen, lung, kidney) was injected into the LC–MS/MS system.

Statistical analysis

All experiments were repeated thrice. Statistical analysis was executed using the SPSS 20.0 software package (SPSS Inc., Chicago, IL, USA), and data were presented as mean \pm SEM. GraphPad Prism 8.0 software (GraphPad Software, San Diego, CA, USA) was used to display the data. The Shapiro–Wilk test was employed to test the normality of the data. The differences between the two groups were evaluated using ANOVA analysis or Student's *t*-tests. The analysis of the categorical variables was conducted using the Mann–Whitney test. $P < 0.05$ was considered statistically significant.

Results

MyD88 up-regulation and spleen impairment in the early *T. spiralis*-infected mice

The western blot results for the 3 d and 5 d groups indicated a significant increase in MyD88 protein levels compared to the 0 d group ($P < 0.05$, Figure 1A). The results signified that *T. spiralis* infection could up-regulate the protein expression of MyD88. Therefore, for the study on early *T. spiralis* infection, we used 5 d to represent the infected stage. Histological results showed that the spleen presented normal morphology, with a clear red pulp (RP) and white pulp (WP) for the control group.

There was also a dense distribution of lymphocytes in RP and WP (Figure 1B). The structure of the spleen corpuscles was damaged in the 5 d group. The interface between WP and RP was blurred, and its arrangement was sparse. Furthermore, the number of lymphocytes was relatively low. Meanwhile, RP displayed hyperplasia (Figure 1B).

To investigate the protective effect of TJ-M2010-5 against pathological damage caused by early *T. spiralis* infection, we conducted histological analysis on the TJ5_5 d group. We found that pre-treatment with TJ-M2010-5 partly reversed these alterations in the WP and RP (Additional file 3). Our findings demonstrate that

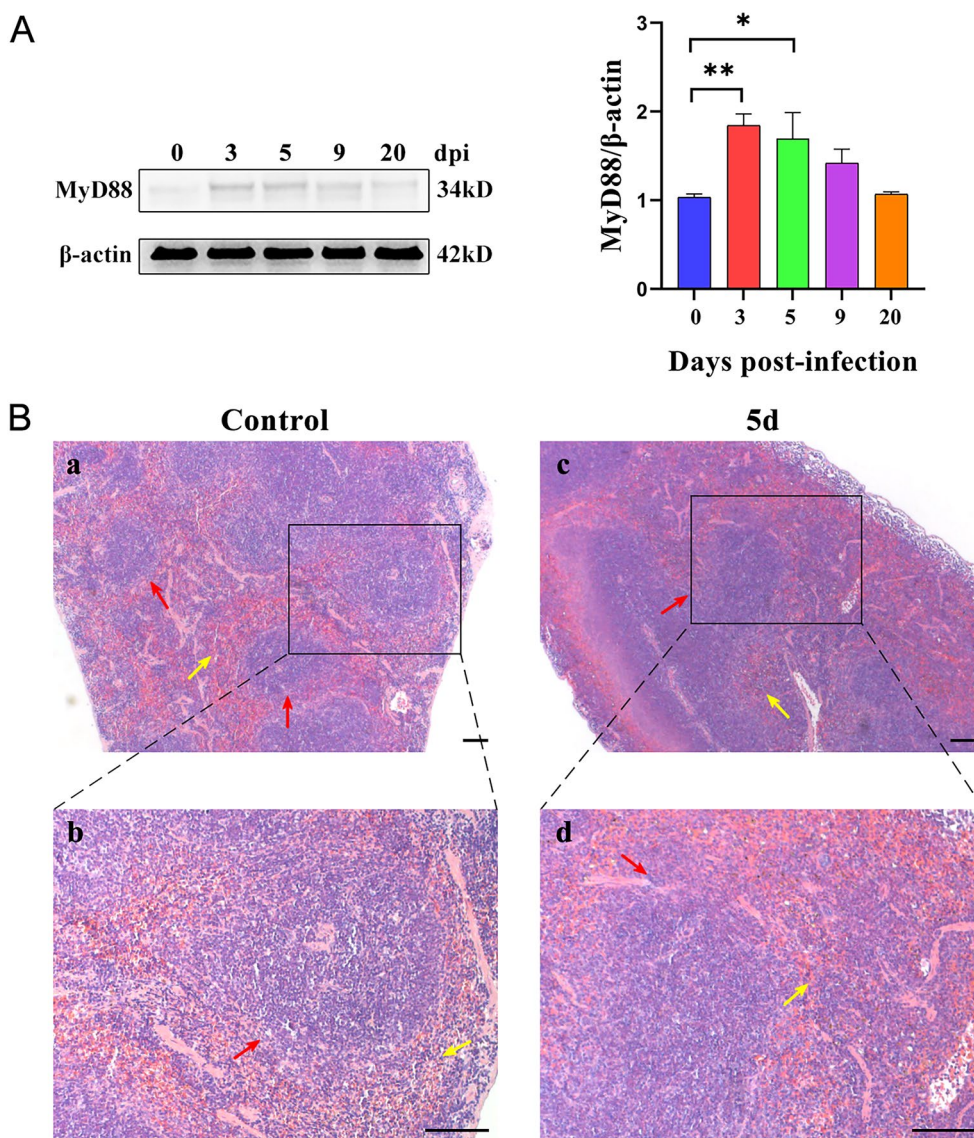


Figure 1 MyD88 upregulation and spleen impairment in the early *T. spiralis*-infected mice. **A** MyD88 protein expression in mice spleen was quantified by western blotting on 0, 3, 5, 9, and 20 dpi, respectively. The protein intensity was analysed by using ImageJ. * $P < 0.05$, ** $P < 0.01$, *** $P < 0.001$. **B** (a) and (b) control group. (c) and (d) 5 d infected group. red arrows: white pulp; yellow arrows: red pulp; Scale bar = 100 μ m.

the up-regulation of MyD88 is a key contributor to the impairment of the spleen caused by trichinella infection.

MyD88 promoter methylation modification and DNMTs/TETs activity

Previous studies have reported that methylation can alter protein expression levels [20, 21]. Therefore, we analysed the changes in methylation levels in the MyD88 promoter region. MethPrimer software predicted that 23 CpG sites were located in the MyD88 promoter region (Figure 2A and B). The agarose gel electrophoresis showed that PCR products were the same size as the target amplified product (250 bp) (Figure 2C). Moreover, the quantitative methylation analysis of the MyD88 promoter revealed that the methylation level of the 5 d group was lower compared to the 0 d group ($P < 0.05$, Figures 2D and E). Interestingly, aside from the C to T mutation, we also discovered a point mutation from G to A (Figure 2F). The levels of DNA mutation significantly increased by 5 dpi, and there was a significant increase in the 5 d group compared to the 0 d group ($P < 0.05$, Figure 2G).

As previously reported, the DNA methylation patterns occurring in CpG motifs were regulated by DNMTs and hydroxymethylases, including the TETs family of dioxygenases [22]. Our results show that the DNMT activity levels significantly decreased in the 5 d group vs the 0 d group ($P < 0.05$) (Figure 2H). Meanwhile, the TET activity levels significantly reduced in the 5 d group vs the 0 d group ($P < 0.05$, Figure 2I). Moreover, the results suggest that DNMTs and TETs can regulate the methylation of the MyD88 promoter, which could lead to an increase in the expression of MyD88 and the activation of downstream inflammatory signalling pathways.

TJ-M2010-5 alleviated inflammation and altered the macrophage phenotype in the early *T. spiralis*-infected mice

The methylation status of the current gene cannot be easily altered with existing drugs [23]; therefore, to reduce inflammation and treat diseases, we opted for MyD88, specifically the TJ-M2010-5 inhibitor, to modify the high expression of MyD88. However, it is unclear whether its expression is regulated by adjusting the methylation level. To further reveal the potential mechanism by which TJ-M2010-5 alleviates inflammation in early *T. spiralis*-infected mice, we conducted a polarisation analysis of M1 and M2 macrophages by flow cytometry. Results showed that the ratio of M1 to M2 macrophages in the spleens of trichinella-infected mice was significantly increased (Figure 3A and B). However, TJ-M2010-5 markedly reduced the ratio of M1 to M2. Edictally, Th1 and Th2 cytokines in the serum of the 0, 5, and TJ5_5 d groups were detected, respectively.

Additionally, *T. spiralis* challenge led to a significant increase in the expression levels of IL-2, IL-12p70, and TNF- α and an insignificant change in the expression levels of IL-4 and IL-13 compared with the 0 d group (Figure 3C). However, TJ-M2010-5 treatment reversed the up-regulated levels of Th1 cytokines (except for TNF- α) and down-regulated the levels of Th2 cytokines. These results demonstrate that TJ-M2010-5 substantially alleviated inflammation in the early *T. spiralis*-infected mice and show that the macrophages' phenotypic switch from M1 to M2 promoted the recovery of the injured spleen.

TJ-M2010-5 altered miRNA expression profile

As the above results demonstrate, MyD88 was more highly expressed in early trichinella infection (5 d group). Accordingly, this study's objective was to perform animal experiments to explore the protective role of TJ-M2010-5 in *T. spiralis*-induced inflammation (Figure 4A).

Through miRNA sequencing, we determined that TJ-M2010-5 markedly alters the miRNA expression profile in different groups. Moreover, differential expression analysis showed that TJ-M2010-5 significantly up-regulated 9 and down-regulated 10 miRNAs compared with the 5 d group (Figure 4B). qPCR results indicated that the expression of miR-340-5p, miR-141-3p, miR-126b-5p, miR-199b-5p, miR-199a-5p, miR-136-5p, miR-10b-5p, miR-221-5p, and miR-21a-3p were all significantly up-regulated.

However, miR-125a-5p, miR-125b-5p, miR-149-5p, miR-18a-3p, miR-3470a, miR-466i-5p, miR-504-5p, miR-664-5p, miR-674-3p, and miR-8112 were all significantly down-regulated in TJ5_5 d group vs the 5 d group. These outcomes were consistent with the RNA-Seq dataset (Figure 4C).

A volcano plot (Figure 4D) illustrates all these DE miRNAs. Gene Ontology (GO) enrichment among the DE miRNAs revealed that they were mainly enriched in terms of regulating cell growth, neuron-to-neuron synapse, GTPase binding, etc. (Figure 4E). Moreover, KEGG enrichment analysis showed that these miRNAs may be associated with the PI3K/AKT signal pathway (Figure 4F).

miR-136-5p targeted and regulated AKT3

After analysing the RNA-Seq results and study reports [24, 25], we determined that miR-136-5p may be involved in the TJ-M2010-5 treatment of spleen impairment during the early stages of *T. spiralis* infection.

To identify potential targets of miR-136-5p, we compared its sequence to the mouse genome database. The results showed that the 3' UTR region of AKT3 contained potential binding sites for the miR-136-5p sequence (Figure 5A). Thus, we transfected miR-136-5p

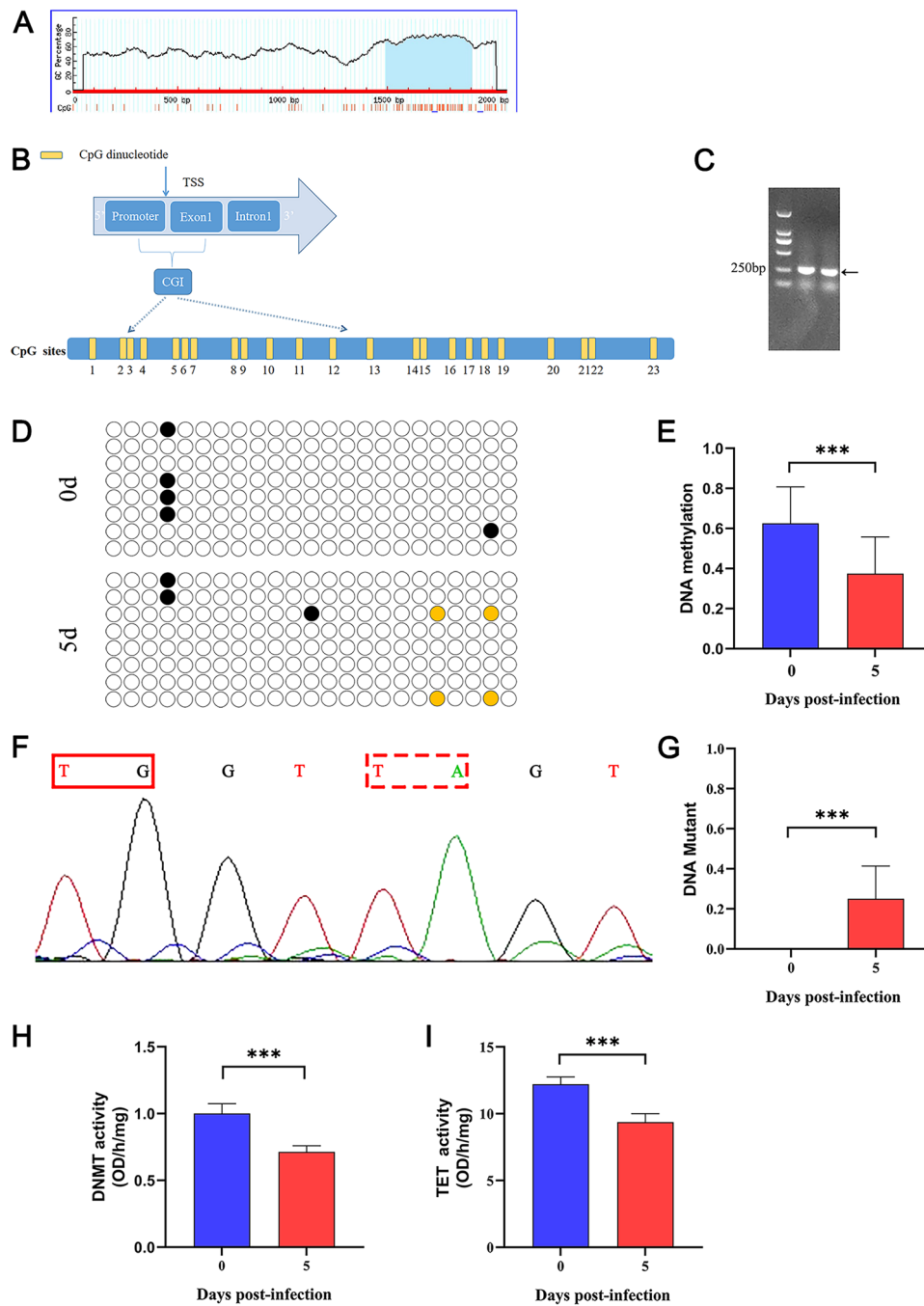


Figure 2 Methylation levels of the MyD88 promoter in mice challenged with *T. spiralis* and DNMTs and TETs activities assays. **A**

MethPrimer software prediction of CGI of the MyD88 promoter region. The blue areas on the picture indicate the potential CGI. **B** The distribution of CpG dinucleotides in the CGI of MyD88. The CGI has a cluster of 23 individual CpG sites, and each yellow rectangle represents a CpG site. **C** The PCR products of MyD88 promoter with methylation primers. **D** The methylation status of the promoter of MyD88 on 0 and 5 dpi, respectively. Each row corresponded to a single template DNA molecule cloned. Eight colonies from each ligation were randomly picked and sequenced. Each circle represented a CpG site (black circles represented methylated CpG site; white circles were unmethylated CpG site; yellow circles were mutant CpG site). **E** The methylation level of the MyD88 promoter on 0 and 5 dpi, respectively. **F** The mutant pattern of the CpG site with G/A mutation. The mutation sites measured by sequencing are framed with red. **G** The mutant level of the MyD88 promoter on 0 and 5 dpi, respectively. **H, I** Bar charts showing DNMTs (**H**) and TETs (**I**) activities of spleen tissues in 0 and 5 dpi, respectively. * $P < 0.05$, ** $P < 0.01$, *** $P < 0.001$.

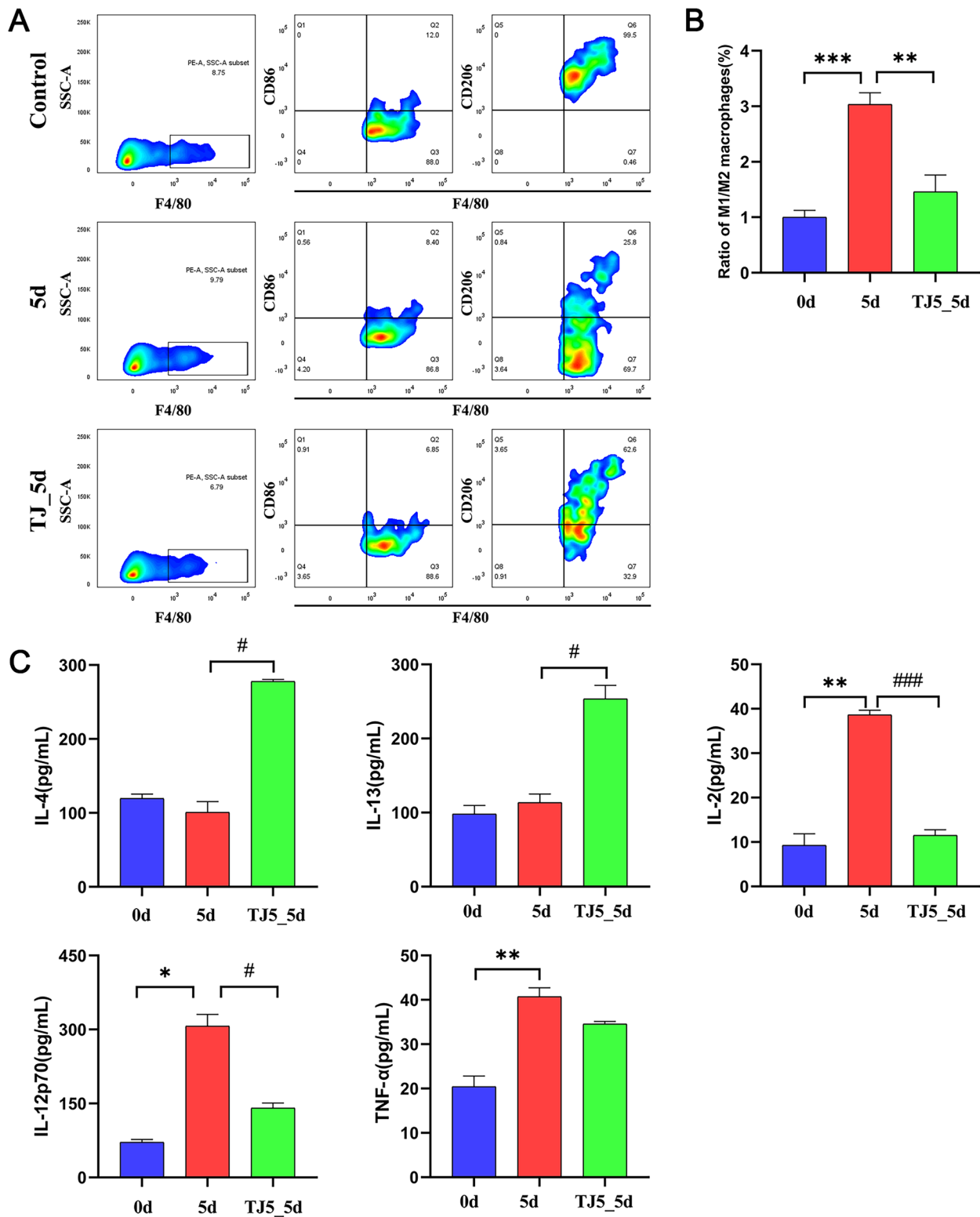


Figure 3 TJ-M2010-5 protective effect on spleen impairment in the early *T. spiralis*-infected mice. **A** Representative plots of M1 and M2 macrophages in the spleens of mice. **B** Flow cytometry in different groups determined the M1/M2 ratio. **C** ELISA analysis of IL-4, IL-13, IL-2, IL-12p70 and TNF- α in the serum from different groups. Compared with 0 d group: * $P < 0.05$, ** $P < 0.01$, *** $P < 0.001$. Compared with 5 d group: # $P < 0.05$, ## $P < 0.01$, ### $P < 0.001$.

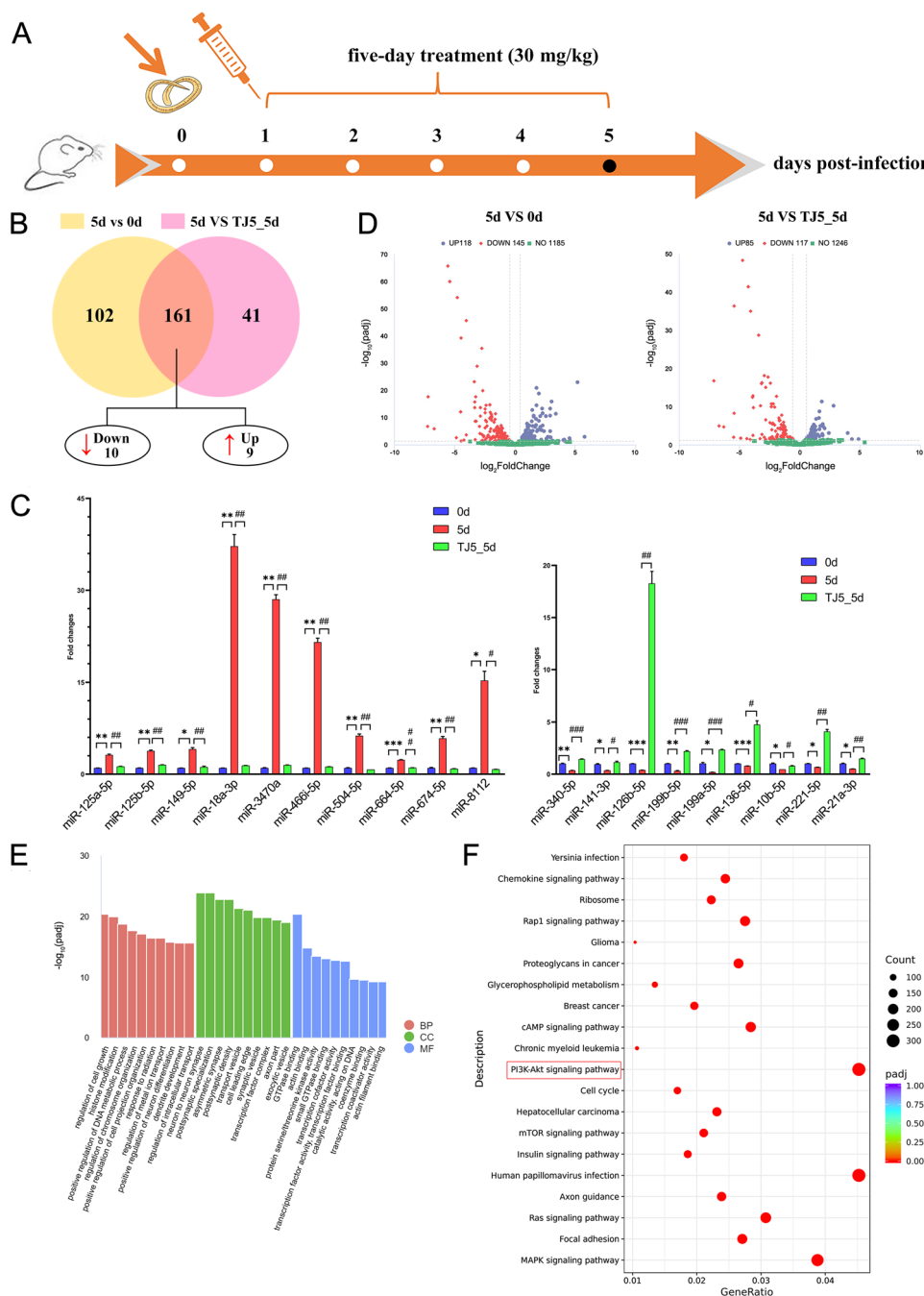


Figure 4 Global view of miRNAs expression profiles in mice spleens during the early infection of *T. spiralis*. **A:** Schematic diagram illustrating the experimental protocols. **B:** Venn diagram showing the intersection of the DE miRNAs among 5 d group vs 0 d group and TJ5_5 d group. **C:** mRNA expression of DE miRNAs in different groups (0, 5 and TJ5_5 d groups) by qPCR. Compared with 0 d group: * $P < 0.05$, ** $P < 0.01$, *** $P < 0.001$. Compared with TJ5_5 d group: # $P < 0.05$, ## $P < 0.01$, ### $P < 0.001$. **D:** Volcano plots of DE miRNAs in 5 d group vs 0 d group (A) and TJ5_5d group (B). Red, higher-expressed miRNAs; Blue, lower-expressed miRNAs. **E–F:** GO (E) and KEGG (F) pathway analysis for DE miRNAs.

mimics into HEK 293 T cells to overexpress miR-136-5p and mimic NC as a control (Figure 5C). The outcomes of the dual-luciferase assay showed that the miR-136-5p mimics+AKT3 WT group suppressed the relative

luciferase activity in HEK 293 T cells. However, the miR-136-5p mimics+AKT3 MUT group did not inhibit the relative luciferase activity. These results confirm that AKT3 is the target gene for miR-136-5p (Figure 5B).

TJ-M2010-5 up-regulated miR-136-5p expression and inhibited the PI3K/AKT3 signalling pathway in RAW264.7 cells

The RAW264.7 cells were pre-treated with six concentrations of TJ-M2010-5 (5, 10, 20, 30, 40, 50 μ M) for 6 h, and the effect of TJ-M2010-5 on inflammation induced by LPS was analysed (Figure 6B). CCK8 assay showed that 20 μ M TJ-M2010-5 had no significant cytotoxicity on RAW264.7 cells (Figure 6A). Therefore, we chose 10 and 20 μ M as the concentration in the subsequent experiments.

The results showed that RAW264.7 cells pre-treated with TJ-M2010-5 significantly inhibited LPS-induced inflammation by down-regulating the expression of IL6, IL1 β , and TNF α (Figure 6C). LPS down-regulated the expression of miR-136-5p, while TJ-M2010-5 reversed these effects (Figure 6D). Furthermore, the ratio of M1 to M2 macrophages was higher in treatment with the LPS group vs the control group (Figures 6F and G). TJ-M2010-5 pre-treatment showed that it could reverse the M1 polarisation of macrophages, decrease the M1/M2 ratio, and inhibit NO production (Figure 6E).

Western blot revealed that LPS treatment did not affect the total expression of PI3K and AKT but did increase the expression of pPI3K, pAKT, AKT3, MyD88, and iNOS. However, TJ-M2010-5 pre-treatment attenuated this effect (Figures 6H and I). Therefore, TJ-M2010-5 can defend against inflammation and exhibits a prominently protective function by down-regulating the expression of IL6, IL1 β , and TNF α . This down-regulating thus reverses the M1 polarisation of macrophages and regulates the PI3K/AKT3 pathways in RAW264.7 cells.

Tissue distribution

For this study, we used liquid chromatography-tandem mass spectrometry (LC-MS/MS) analysis to quantify the deposition of TJ-M2010-5 in major organs of the mice. The calibration curves, correlation coefficients, and linear ranges of TJ-M2010-5 are provided in Additional files 4–6.

TJ-M2010-5 presented a good linearity ($R^2 > 0.99$), with concentrations between 50 and 1000 ng/mL. At 30 min after administration, the concentration of TJ-M2010-5 in the tissues was ranked high to low as follows: liver > spleen > lung > kidney (Figure 7A).

At 2 h after administration, the concentration of TJ-M2010-5 in the tissues remained in the same order: liver > spleen > lung > kidney. At 6 h after administration, the same concentration order was retained. However, 12 h after administration, the concentration changed to spleen > liver > lung > kidney. At 48 h after administration, the concentration again displayed the order:

liver > spleen > lung > kidney. The results suggested that TJ-M2010-5 is hepatosplenic-targeted.

Discussion

Previous studies have shown that TLR receptors activate the innate immune system and trigger downstream signalling molecules to participate in immune regulation [26]. Han et al. revealed that the MyD88 expression changes during *T. spiralis* infection can affect the secretion of the macrophages inflammatory cytokines and lead to immune suppression [27]. A previous study reported that MyD88-deficient mice display a complete loss in resistance to acute infection of *T. gondii* [28]. Studies have also shown that this adaptor protein's dysfunction may negatively affect the systemic and local immune response depending on MyD88 expression [29].

Typically, *T. spiralis* infection can activate Th1/Th2 mediated immune response and sustain a long-term inflammatory state in the infection host [30, 31]. In this study, we observed that the spleen tissue of the early *T. spiralis*-infected mice was damaged in the 5 d group. Similarly, we found that the protein expression level of MyD88 was highly expressed in the 5 d group compared with the control group. To further explore this immune imbalance, we assayed the MyD88 promoter region methylation status of spleen tissues after *T. spiralis* infection. Generally, cancer cells have both regional hypermethylation (aberrant DNA methylation) and global hypomethylation [32].

Our study found that MyD88 methylation in mice infected with *T. spiralis* aligned with humans exposed to *H. pylori*-triggered chronic inflammation and colorectal cancer [33, 34]. Previous studies have revealed that regulating gene transcription through DNA methylation is related to the development of various diseases [35–37]. We observed that the methylation status of the MyD88 promoter was significantly decreased in *T. spiralis*-infected mice compared with the 0 d group. Theoretically, the hypermethylation status of DNA sequences is related to the inhibition of gene expression [38, 39].

Interestingly, we also found G to A point mutants. Previous studies have reported that DNA hypomethylation can lead to elevated mutation rates [40, 41], mainly G/A mutations, due to the strong spontaneous deamination and cellular DNA repair machinery [42]. Due to the dynamic transition, gene expression regulation is very sophisticated [43, 44]. Finally, differences in methylation can partially account for the up-regulation of MyD88 protein expression. The changes in the spleen tissues of the early *T. spiralis*-infected mice should be considered.

Furthermore, DNMTs and TETs regulate DNA methylation at specific sites [45, 46]. Importantly, growing evidence indicates that TETs and DNMTs can also alter the

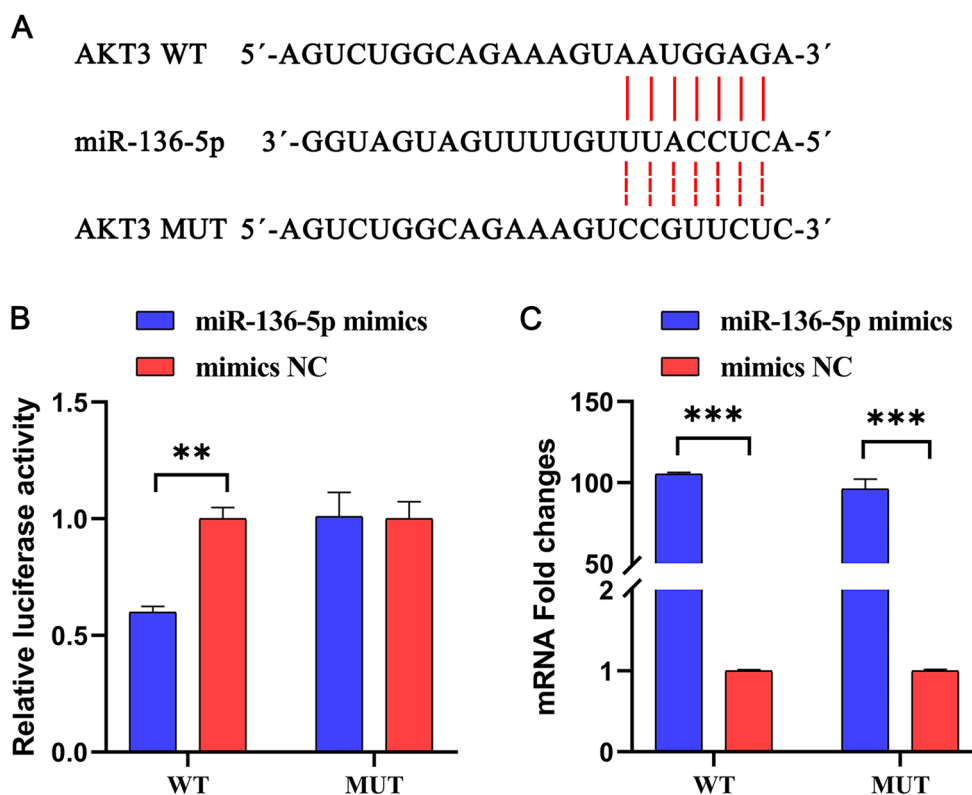


Figure 5 miR-136-5p targeted and regulated AKT3. **A** miR-136-5p and complementary AKT3 nucleotide sequence. **B** Assay results of dual-luciferase. **C** Relative expression levels of miR-136-5p in HEK 293 T cells after transfection with miR-136-5p mimics and mimics NC.

expression of important host genes involved in immune responses [47, 48]. In this study, we observed that the enzyme activity of DNMTs and TETs was decreased in the 5 d group vs the 0 d group ($P < 0.05$). Therefore, we hypothesised that the variation in methylation ratios of MyD88 could be partially due to the reduction of DNMTs and TETs function (enzymatic and nonenzymatic activities) [49]. This finding aligns with the findings reported by Zhang et al. [50].

Typically, high MyD88 expression activates the inflammatory signalling pathways after 5 days of trichinella infection [23]. To reduce inflammation and treat the diseases, we selected the MyD88 inhibitor TJ-M2010-5 to interrupt the activation of the inflammatory signalling pathways induced by high MyD88 expression. In the early infection stage, macrophages were predominantly M1, contributing to the inflammatory response and promoting the elimination of worms [8]. Earlier studies have confirmed macrophage TLRs to be involved in pathogen recognition and immune regulation [51]. In our study, a large number of M1-phenotype splenic macrophages were activated after *T. spiralis* infection. TJ-M2010-5 treatment significantly decreased this activation while inducing the transformation of the M1 to the M2

macrophages. TJ-M2010-5 also positively contributed to the decrease of IL-2 and IL-12p70, the up-regulation of IL-4 and IL-13, and the attenuation of the inflammatory response in vivo. However, TJ-M2010-5 did not affect TNF- α levels and insignificantly contributed to the systemic anti-inflammatory response.

Subsequently, we found that TJ-M2010-5 markedly altered the miRNA expression profile in the early *T. spiralis*-infected mice. Notably, the TJ-M2010-5-related differentially expressed miRNAs targeted the PI3K/AKT signalling pathway. Numerous reports have shown that the PI3K/AKT pathway is involved in the mechanisms of inflammation and is a potential target for anti-inflammation therapy [52–54].

Moreover, AKT3 is vital in growth, proliferation, and metabolism and is dysregulated in some oncological diseases [55]. Previous studies have demonstrated that TLR4 initiates the microglia by triggering MyD88 and activating the downstream PI3K/AKT signalling pathway [56]. Yin et al. reported that LPS can remodel the tumour microenvironment and promote the anti-tumour effect via TLR4/MyD88/AKT/NF- κ B pathway in pancreatic cancer [57].

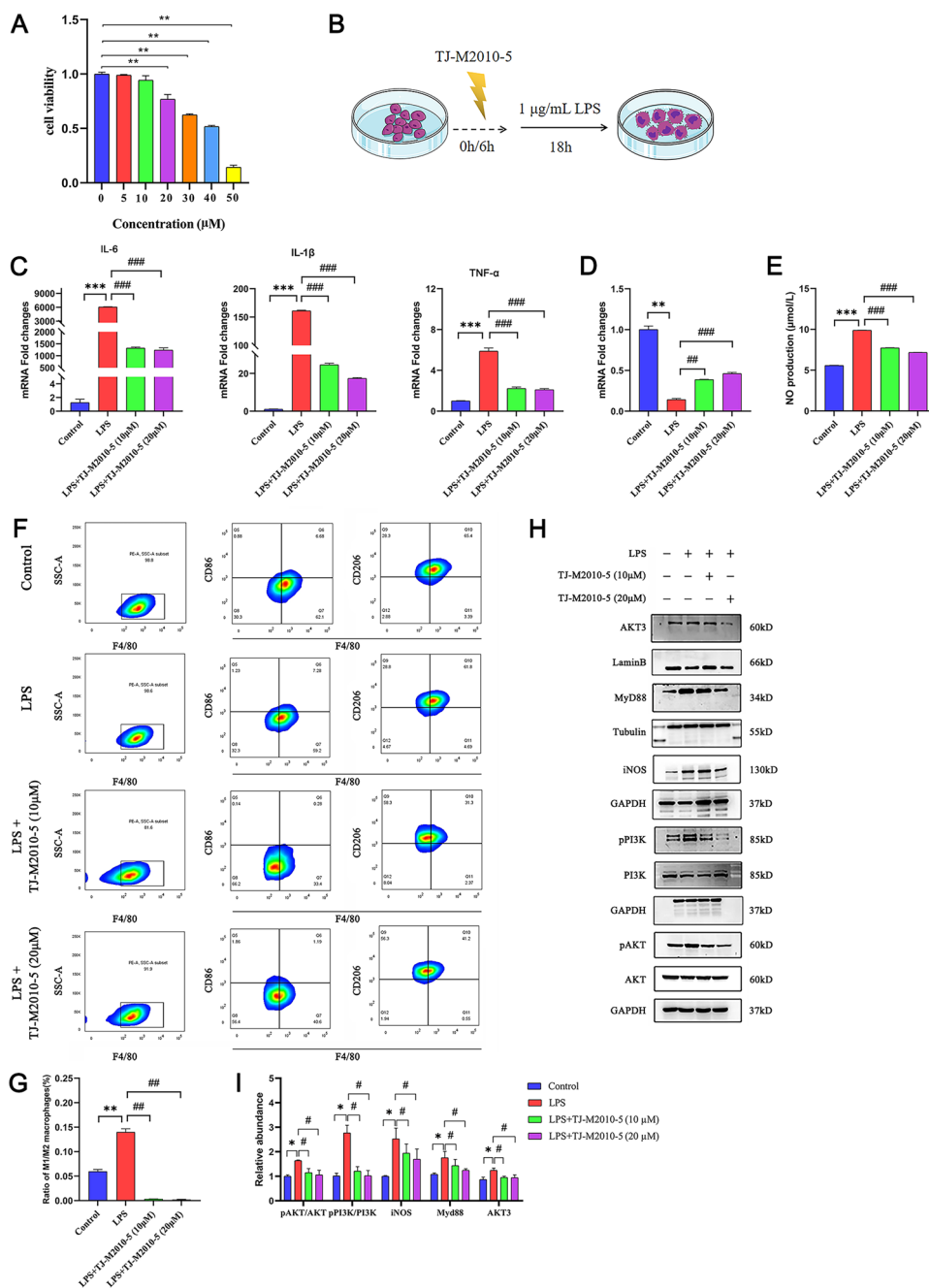


Figure 6 TJ-M2010-5 reduced inflammation on RAW264.7 cells stimulated with LPS. **A** CCK8 assay. * $P < 0.05$, ** $P < 0.01$, *** $P < 0.001$. **B** Schematic diagram of RAW264.7 inflammatory cell model induced by LPS. **C** IL-6, IL-1β and TNF-α mRNA expression of different groups. **D** miR-136-5p mRNA expression of different groups. **E** TJ-M2010-5 effects on the NO production in RAW264.7 cells stimulated by LPS. **F, G** Representative plots of M1 and M2 macrophages pre-treatment with 10 and 20 μM TJ-M2010-5. The M1/M2 ratio was determined by flow cytometry. **H-I** Western blotting analysis of iNOS, pPI3K, PI3K, pAKT, AKT, MyD88 and AKT3 protein expression. The protein intensity was analysed by using ImageJ. Compared with control group: * $P < 0.05$, ** $P < 0.01$, *** $P < 0.001$; Compared with LPS group: # $P < 0.05$, ## $P < 0.01$, ### $P < 0.001$.

However, the role of AKT3 in MyD88-mediated function during early *T. spiralis* infection, specifically in spleen impairment, is poorly understood. Furthermore, miR-136-5p, as a tumour suppressor, plays an important

role in regulating various cellular processes [58], inhibiting viability, proliferation, migration, and invasion, and promoting apoptosis of tumour cells [59]. In this study, we detected that the mRNA expression of miR-136-5p

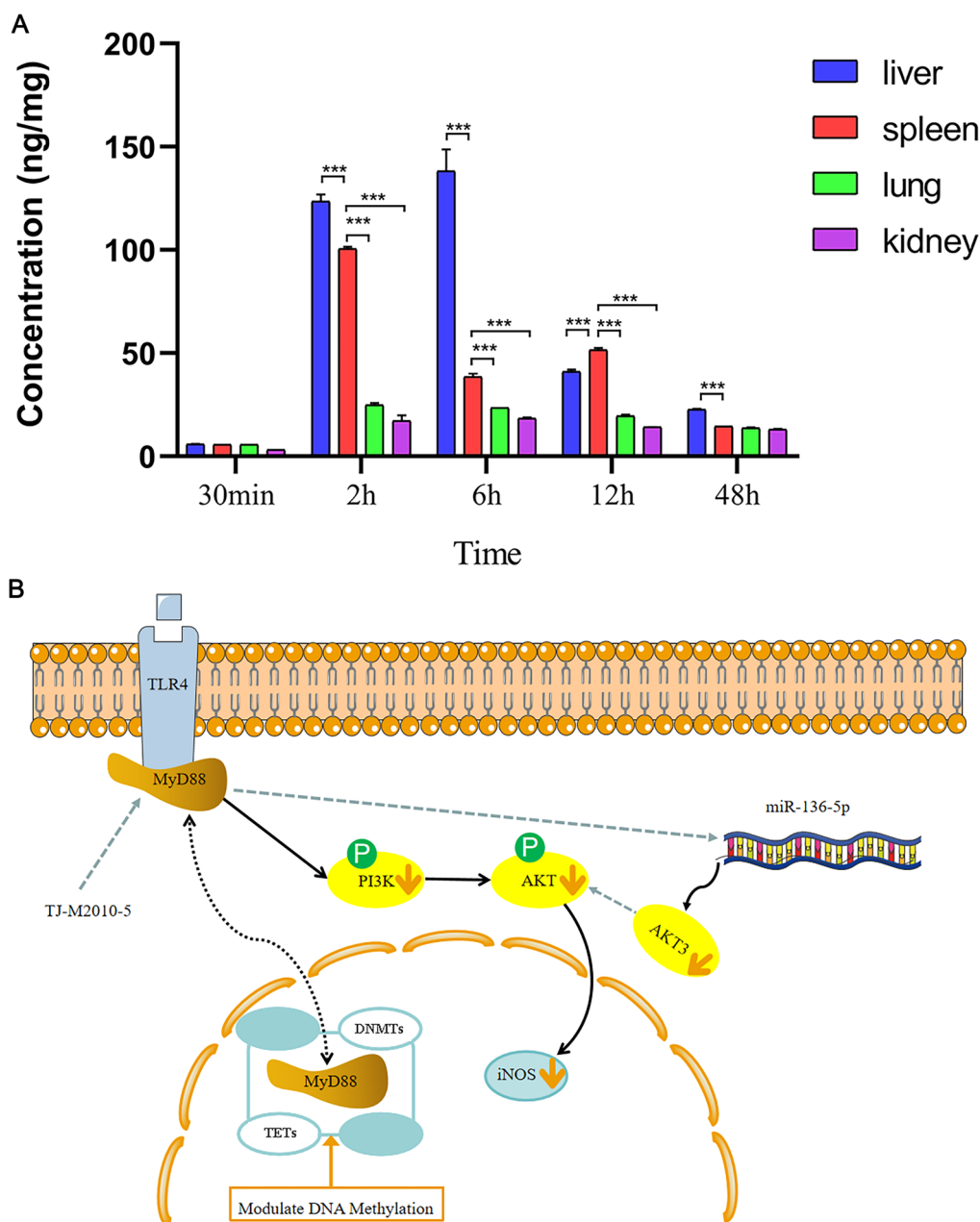


Figure 7 Tissue distribution and scheme summarizing the protective effects of TJ-M2010-5 in spleen impairment. **A** Concentration of TJ-M2010-5 in different tissues collected at 30 min, 2, 6, 12 and 48 h after 30 mg/kg TJ-M2010-5 treatment. * $P < 0.05$, ** $P < 0.01$, *** $P < 0.001$. **B** A schematic diagram of TJ-M2010-5 modulating the inflammatory response via PI3K/AKT3 pathway in spleen impairment.

was significantly up-regulated in TJ-M2010-5-pre-treated RAW264.7 cells and the spleens of TJ5_5 d mice. The study’s luciferase reporter assays identified AKT3 as a target on miR-136-5p. Some drugs or compounds enhanced their anti-inflammatory effects by inhibiting AKT3 expression [60–63].

Macrophages are involved in many parasitic infections [7, 64]. TLR4 on the surface of macrophages plays an

important role in innate immunity between parasites and hosts [65–67]. As a TLR4 agonist associated with parasite immunology, the LPS-stimulated macrophage model is ideal and instructive for studying the polarisation of M1 to M2 in vitro.

When LPS is stimulated, macrophages can release a variety of inflammatory factors, such as TNF- α , IL-6, NO, and IL-1 β . NO is an important mediator of inflammation

amplification. It is produced by nitric oxide synthase (NOS), and the inducible NOS (iNOS) is expressed in various cells, such as macrophages and dendritic cells. NO has assorted biological functions in mammalian cells, including microbial immunity, vasodilation, and the regulation of cell signal transduction [68]. Overproduction of NO may lead to tissue damage and worsen inflammatory conditions. Thus, controlling NO production can alleviate inflammation symptoms. Our investigation indicated that TJ-M2010-5 alleviated inflammation. In addition, it reversed the effect in RAW264.7 cells by activating the PI3K/AKT3 pathway induced by LPS and overexpressing IL-6, IL-1 β , TNF- α , NO, and iNOS.

Furthermore, M1 and M2 macrophages are commonly considered pro-inflammatory or anti-inflammatory regulatory properties, respectively. This study showed that TJ-M2010-5 exerted its anti-inflammatory effects by regulating the levels of inflammatory factors and promoting the polarisation of M1 to M2. Consistent with our findings, TJ-M2010-5 can regulate RAW264.7 cell inflammation by inhibiting AKT3 expression. However, from a preliminary perspective of miRNA profile analysis, TJ-M2010-5 affected the expression of multiple miRNAs. Thus, it needs to be investigated whether the effect is produced via additional mechanisms and targets. It is worth mentioning that AKT3 may not be the unique target of miR-136-5p, and more experiments are needed.

In addition, a significant level of TJ-M2010-5 was found in the liver and spleen, likely due to its uptake by the reticuloendothelial system (RES) phagocytic cells [69]. The study showed that TJ-M2010-5 played a negative feedback regulatory role (Figure 7B) in the inflammation signalling pathway. Our outcomes suggest that administering TJ-M2010-5 could facilitate the resolution of the pro-inflammatory state of macrophages and promote the functional improvement of spleen immunity function.

Nonetheless, our research has limitations since DNA methylation differs across cell types within the same tissue. Consequently, MyD88 hypomethylation seems specific to both cell type and tissue in our study. Furthermore, we confirmed that TJ-M2010-5 could reduce inflammation, but we did not verify its involvement in the anti-inflammatory process through the PI3K/AKT3 signalling pathway in vivo experiments. Finally, increasing the sample size of experimental animals is recommended for further research. Therefore, additional, comprehensive studies should be conducted to address these limitations more effectively.

In conclusion, we revealed that TJ-M2010-5 significantly alleviated inflammation in RAW264.7 cells by blocking PI3K/miR-136-5p/AKT3 activation and promoting macrophage polarisation towards M2. The results suggested that MyD88 up-regulation was altered

by its methylation in the early *T. spiralis*-infected mice, with DNMTs and TETs being the major enzymes involved. Furthermore, this study demonstrated the protective effect of TJ-M2010-5 in the early *T. spiralis*-infected mice model, which relieved Th1 cytokine secretion, increased Th2 cytokine secretion and promoted splenic macrophage polarisation towards M2. Therefore, we propose that TJ-M2010-5 is a promising therapeutic agent that might provide a clinical alternative for treating inflammation-related diseases caused by parasite infection.

Supplementary Information

The online version contains supplementary material available at <https://doi.org/10.1186/s13567-025-01459-2>.

Additional file 1. Primer sequence of target and reference genes.

Additional file 2. Antibodies used in this study.

Additional file 3. TJ-M2010-5 protective effect on spleen impairment in *T. spiralis* infected mice.

Additional file 4. Positive mode electrospray ionisation (ESI) mass spectrum of TJ-M2010-5.

Additional file 5. Total ion chromatogram (TIC) of TJ-M2010-5.

Additional file 6. Calibration curve, correlation coefficients and linear ranges of TJ-M2010-5.

Acknowledgements

The authors would like to acknowledge the team members of the Zoonoses Laboratory at Jilin University for their careful guidance.

Authors' contributions

Conceptualisation, XLW; Methodology, HFB, QQD and GLC; Software, HFB and XXW; Formal Analysis, HFB, GLC and SYZ; Investigation, HFB, LFX and SNW; Data Curation, QQD, NJ and XXW; Writing—Original Draft Preparation, HFB, SNW and GLC; Writing—Review and Editing, XLW; Project Administration, XLW. All authors read and approved the final manuscript.

Funding

This work was supported by Grants from the Jilin Province Key Research and Development Program of China (20230202086NC).

Data availability

All data generated during this study are included in this published article and its supplementary information files.

Declarations

Ethics approval and consent to participate

All mice were raised and handled strictly following the National Institutes of Health guide for the care and use of laboratory animals and approved by the Ethics Committee for Animal Experiments of Jilin University (NO. 202201-104, date: 25/2/2022).

Competing interests

The authors declare that they have no competing interests.

Author details

¹State Key Laboratory for Diagnosis and Treatment of Severe Zoonotic Infectious Diseases, Key Laboratory for Zoonosis Research of the Ministry of Education, Institute of Zoonosis, and College of Veterinary Medicine, Jilin University, Changchun 130062, China.

Received: 20 August 2024 Accepted: 30 September 2024
Published online: 04 February 2025

References

- Elgendy DI, Othman AA, Hasby Saad MA, Soliman NA, Mwafy SE (2020) Resveratrol reduces oxidative damage and inflammation in mice infected with *Trichinella spiralis*. *J Helminthol* 94:e140
- Lind NA, Rael VE, Pestal K, Liu B, Barton GM (2022) Regulation of the nucleic acid-sensing Toll-like receptors. *Nat Rev Immunol* 22:224–235
- Janssens S, Beyaert R (2002) A universal role for MyD88 in TLR/IL-1R-mediated signaling. *Trends Biochem Sci* 27:474–482
- Chen J, Ullah H, Zheng Z, Gu X, Su C, Xiao L, Wu X, Xiong F, Li Q, Zha L (2020) Soyasaponins reduce inflammation by downregulating MyD88 expression and suppressing the recruitments of TLR4 and MyD88 into lipid rafts. *BMC Complement Med Ther* 20:167
- Ma KN, Zhang Y, Zhang ZY, Wang BN, Song YY, Han LL, Zhang XZ, Long SR, Cui J, Wang ZQ (2023) *Trichinella spiralis* galectin binding to toll-like receptor 4 induces intestinal inflammation and mediates larval invasion of gut mucosa. *Vet Res* 54:113
- Zhang R, Zhang Y, Yan SW, Cheng YK, Zheng WW, Long SR, Wang ZQ, Cui J (2024) Galactomannan inhibits *Trichinella spiralis* invasion of intestinal epithelium cells and enhances antibody-dependent cellular cytotoxicity related killing of larvae by driving macrophage polarization. *Parasite* 31:6
- Coakley G, Harris NL (2020) Interactions between macrophages and helminths. *Parasite Immunol* 42:e12717
- Liu RD, Meng XY, Le Li C, Xu QY, Lin XZ, Dong BR, Ye CY, Miao TT, Si XY, Long SR, Cui J, Wang ZQ (2023) *Trichinella spiralis* cathepsin L induces macrophage M1 polarization via the NF- κ B pathway and enhances the ADCC killing of newborn larvae. *Parasites Vectors* 16:433
- Yan SW, Zhang R, Guo X, Wang BN, Long SR, Liu RD, Wang ZQ, Cui J (2023) *Trichinella spiralis* dipeptidyl peptidase 1 suppressed macrophage cytotoxicity by promoting M2 polarization via the STAT6/PPAR γ pathway. *Vet Res* 54:77
- Sato F, Tsuchiya S, Meltzer SJ, Shimizu K (2011) MicroRNAs and epigenetics. *FEBS J* 278:1598–1609
- Ko EK, Capell BC (2021) Methyltransferases in the pathogenesis of keratinocyte cancers. *Cancers* 13:3402
- Hewezi T (2020) Epigenetic mechanisms in nematode-plant interactions. *Annu Rev Phytopathol* 58:119–138
- Russo F, Di Bella S, Bonnici V, Laganà A, Rainaldi G, Pellegrini M, Pulvirenti A, Giugno R, Ferro A (2014) A knowledge base for the discovery of function, diagnostic potential and drug effects on cellular and extracellular miRNAs. *BMC Genomics* 15:54
- He X, Pan W (2022) Host-parasite interactions mediated by cross-species microRNAs. *Trends Parasitol* 38:478–488
- Yang H, Zhou P, Li Q, Zhou X, Li J, Wang J, Wang J, Zhao Y, Yang B, Zhang B, Dai C, Zou Z, Yang Y, Chen Z (2022) TJ-M2010-5 attenuates severe myocardial ischemia/reperfusion injury in heart transplantation by inhibiting MyD88 homodimerization in vivo. *J Cardiovasc Transl* 15:1366–1376
- Liu H, Ji M, Bi Y, Xiao P, Zhao J, Gou J, Yin T, He H, Ding H, Tang X, Zhang Y (2023) Integration of MyD88 inhibitor into mesoporous cerium oxide nanozymes-based targeted delivery platform for enhancing treatment of ulcerative colitis. *J Control Release* 361:493–509
- Anders S, Huber W (2010) Differential expression analysis for sequence count data. *Genome Biol* 11:R106
- Friedländer MR, Mackowiak SD, Li N, Chen W, Rajewsky N (2012) miR-Deep2 accurately identifies known and hundreds of novel microRNA genes in seven animal clades. *Nucleic Acids Res* 40:37–52
- Storey J (2003) The positive false discovery rate: a bayesian interpretation and the Q-value. *Ann Stat* 31:2013–2035
- Moore LD, Le T, Fan G (2013) DNA methylation and its basic function. *Neuropsychopharmacology* 38:23–38
- Dabe EC, Sanford RS, Kohn AB, Bobkova Y, Moroz LL (2015) DNA methylation in basal metazoans: insights from ctenophores. *Integr Comp Biol* 55:1096–1110
- Lee J, Song JH, Park JH, Chung MY, Lee SH, Jeon SB, Park SH, Hwang JT, Choi HK (2023) Dnmt1/Tet2-mediated changes in CpG methylation regulate the development of nonalcoholic fatty liver disease by controlling the Gbp2-Ppar γ -CD36 axis. *Exp Mol Med* 55:143–157
- Liu YC, Kwon J, Fabiani E, Xiao Z, Liu YV, Follo MY, Liu J, Huang H, Gao C, Liu J, Falconi G, Valentini L, Gurnari C, Finelli C, Cocco L, Liu JH, Jones AI, Yang J, Yang H, Thoms JAI, Unnikrishnan A, Pimanda JE, Pan R, Bassal MA, Voso MT, Tenen DG, Chai L (2022) Demethylation and up-regulation of an oncogene after hypomethylating therapy. *N Engl J Med* 386:1998–2010
- Gao Z, Li Q, Zhang Y, Gao X, Li H, Yuan Z (2020) Ripasudil alleviated the inflammation of RPE cells by targeting the miR-136-5p/ROCK/NLRP3 pathway. *BMC Ophthalmol* 20:134
- Ding H, Ye ZH, Wen DY, Huang XL, Zeng CM, Mo J, Jiang YQ, Li JJ, Cai XY, Yang H, Chen G (2017) Downregulation of miR-136-5p in hepatocellular carcinoma and its clinicopathological significance. *Mol Med Rep* 16:5393–5405
- Saikh KU (2021) MyD88 and beyond: a perspective on MyD88-targeted therapeutic approach for modulation of host immunity. *Immunol Res* 69:117–128
- Han C, Xu J, Liu CH, Li X, Zhai P, Hashan A, Song M (2018) Modulation of TLR2 and TLR4 in macrophages following *Trichinella Spiralis* infection. *Helminthologia* 55:195–203
- Scanga CA, Aliberti J, Jankovic D, Tilloy F, Bennouna S, Denkers EY, Medzhitov R, Sher A (2002) Cutting edge: MyD88 is required for resistance to *Toxoplasma gondii* infection and regulates parasite-induced IL-12 production by dendritic cells. *J Immunol* 168:5997–6001
- Barboza R, Reis AS, da Silva LG, Hasenkamp L, Pereira KR, Câmara NO, Costa FT, Lima MR, Alvarez JM, Boscardin SB, Epiphanyo S, Marinho CR (2014) MyD88 signaling is directly involved in the development of murine placental malaria. *Infect Immun* 82:830–838
- Ilic N, Gruden-Movsesijan A, Sofronic-Milosavljevic L (2012) *Trichinella spiralis*: shaping the immune response. *Immunol Res* 52:111–119
- Saracino MP, Vila CC, Cohen M, Gentilini MV, Falduto GH, Calcagno MA, Roux E, Venturiello SM, Malchiodi EL (2020) Cellular and molecular changes and immune response in the intestinal mucosa during *Trichinella spiralis* early infection in rats. *Parasit Vectors* 13:505
- Robertson KD (2005) DNA methylation and human disease. *Nat Rev Genet* 6:597–610
- Vafadar-Isfahani N, Parr C, McMillan LE, Sanner J, Yeo Z, Saddington S, Peacock O, Cruickshanks HA, Meehan RR, Lund JN, Tufarelli C (2017) Decoupling of DNA methylation and activity of intergenic LINE-1 promoters in colorectal cancer. *Epigenetics* 12:465–475
- Yoshida T, Yamashita S, Takamura-Enya T, Niwa T, Ando T, Enomoto S, Maekita T, Nakazawa K, Tatematsu M, Ichinose M, Ushijima T (2011) Alu and Sata hypomethylation in *Helicobacter pylori*-infected gastric mucosae. *Int J Cancer* 128:33–39
- Zhang M, Gao Y, Li Q, Cao H, Yang J, Cai X, Xiao J (2022) Downregulation of DNA methyltransferase-3a ameliorates the osteogenic differentiation ability of adipose-derived stem cells in diabetic osteoporosis via Wnt/ β -catenin signaling pathway. *Stem Cell Res Ther* 13:397
- Knight HM, Demirbugen ÖZ M, PerezGrovas-Saltijeral A (2024) Dysregulation of RNA modification systems in clinical populations with neurocognitive disorders. *Neural Regen Res* 19:1256–1261
- Elmuti L, Amundson J, Oberman E, Kamat A, Sedig L, Lastra RR, Aldape K, Quezado M, Pratt DW, Cimino PJ, Abdullaev Z, Pytel P, Applebaum MA, Bennett JA (2024) Diffuse pediatric-type high-grade glioma arising in an ovarian mature cystic teratoma. *Int J Gynecol Pathol* 43:90–96
- Razin A, Riggs AD (1980) DNA methylation and gene function. *Science* 210:604–610
- Chen Q, Yan W, Duan E (2016) Epigenetic inheritance of acquired traits through sperm RNAs and sperm RNA modifications. *Nat Rev Genet* 17:733–743
- Chen RZ, Pettersson U, Beard C, Jackson-Grusby L, Jaenisch R (1998) DNA hypomethylation leads to elevated mutation rates. *Nature* 395:89–93
- Zhang Y, Wendte JM, Ji L, Schmitz RJ (2020) Natural variation in DNA methylation homeostasis and the emergence of epialleles. *Proc Natl Acad Sci U S A* 117:4874–4884
- Shang X, Su J, Wan Q, Su J, Feng X (2014) CpG methylation in the 5'-flanking region of LGP2 gene lacks association with resistance/susceptibility to GCRV but contributes to the differential expression between muscle and spleen tissues in grass carp, *Ctenopharyngodon idella*. *Fish Shellfish Immunol* 40:154–163

43. Strober BJ, Elorbany R, Rhodes K, Krishnan N, Tayeb K, Battle A, Gilad Y (2019) Dynamic genetic regulation of gene expression during cellular differentiation. *Science* 364:1287–1290
44. Lugagne J-B, Blassick CM, Dunlop MJ (2024) Deep model predictive control of gene expression in thousands of single cells. *Nat Commun* 15:2148
45. Jones PA (2012) Functions of DNA methylation: islands, start sites, gene bodies and beyond. *Nat Rev Genet* 13:484–492
46. Tahiliani M, Koh KP, Shen Y, Pastor WA, Bandukwala H, Brudno Y, Agarwal S, Iyer LM, Liu DR, Aravind L, Rao A (2009) Conversion of 5-methylcytosine to 5-hydroxymethylcytosine in mammalian DNA by MLL partner TET1. *Science* 324:930–935
47. Pacis A, Tailleux L, Morin AM, Lambourne J, Maclsaac JL, Yotova V, Dumaine A, Danckaert A, Luca F, Grenier JC, Hansen KD, Gicquel B, Yu M, Pai A, He C, Tung J, Pastinen T, Kobor MS, Pique-Regi R, Gilad Y, Barreiro LB (2015) Bacterial infection remodels the DNA methylation landscape of human dendritic cells. *Genome Res* 25:1801–1811
48. Anier K, Urb M, Kipper K, Herodes K, Timmusk T, Zharkovsky A, Kalda A (2018) Cocaine-induced epigenetic DNA modification in mouse addiction-specific and non-specific tissues. *Neuropharmacology* 139:13–25
49. Chen W, Liu N, Shen S, Zhu W, Qiao J, Chang S, Dong J, Bai M, Ma L, Wang S, Jia W, Guo X, Li A, Xi J, Jiang C, Kang J (2021) Fetal growth restriction impairs hippocampal neurogenesis and cognition via Tet1 in offspring. *Cell Rep* 37:109912
50. Zhang D, An X, Li Z, Zhang S (2019) Role of gene promoter methylation regulated by TETs and DNMTs in the overexpression of HLA-G in MCF-7 cells. *Exp Ther Med* 17:4709–4714
51. Mazumder S, Sinha A, Ghosh S, Sharma GC, Prusty BM, Manna D, Pal D, Pal C, Dasgupta S (2023) *Leishmania* LPG interacts with LRR5/LRR6 of macrophage TLR4 for parasite invasion and impairs the macrophage functions. *Pathog Dis* 81:ftad019
52. Kim SM, Park S, Hwang SH, Lee EY, Kim JH, Lee GS, Lee G, Chang DH, Lee JG, Hwang J, Lee Y, Kyung M, Kim EK, Kim JH, Kim TH, Moon JH, Kim BC, Ko G, Kim SY, Ryu JH, Lee JS, Lee CH, Kim JY, Kim S, Lee WJ, Kim MH (2023) Secreted *Akkermansia muciniphila* threonyl-tRNA synthetase functions to monitor and modulate immune homeostasis. *Cell Host Microbe* 31:1021–1037
53. Han Y, Guo S, Li Y, Li J, Zhu L, Liu Y, Lv Y, Yu D, Zheng L, Huang C, Li C, Hu J, Liu Z (2023) Berberine ameliorate inflammation and apoptosis via modulating PI3K/AKT/NFκB and MAPK pathway on dry eye. *Phytomedicine* 121:155081
54. Fang Z, Yushanjiang F, Wang G, Zheng X, Jiang X (2023) Germacrone mitigates cardiac remodeling by regulating PI3K/AKT-mediated oxidative stress, inflammation, and apoptosis. *Int Immunopharmacol* 124:110876
55. Dong Y, Liang G, Yuan B, Yang C, Gao R, Zhou X (2015) MALAT1 promotes the proliferation and metastasis of osteosarcoma cells by activating the PI3K/Akt pathway. *Tumour Biol* 36:1477–1486
56. Rahimifard M, Maqbool F, Moeini-Nodeh S, Niaz K, Abdollahi M, Braidy N, Nabavi SM, Nabavi SF (2017) Targeting the TLR4 signaling pathway by polyphenols: a novel therapeutic strategy for neuroinflammation. *Ageing Res Rev* 36:11–19
57. Yin H, Pu N, Chen Q, Zhang J, Zhao G, Xu X, Wang D, Kuang T, Jin D, Lou W, Wu W (2021) Gut-derived lipopolysaccharide remodels tumoral micro-environment and synergizes with PD-L1 checkpoint blockade via TLR4/MyD88/AKT/NF-κB pathway in pancreatic cancer. *Cell Death Dis* 12:1033
58. Hsu CY, Allela OQB, Mahdi SA, Doshi OP, Adil M, Ali MS, Saadh MJ (2023) miR-136-5p: a key player in human cancers with diagnostic, prognostic and therapeutic implications. *Pathol Res Pract* 250:154794
59. Zhang M, Xu T, Tong D, Yu X, Liu B, Jiang L, Liu K (2024) MiR-136-5p in cancer: roles, mechanisms, and chemotherapy resistance. *Gene* 909:148265
60. Sun KH, Lee MY, Jeon YJ (2023) Inhibition of phagocytosis by silibinin in mouse macrophages. *Curr Issues Mol Biol* 45:8126–8137
61. Payne A, Taka E, Adinew GM, Soliman KFA (2023) Molecular mechanisms of the anti-inflammatory effects of epigallocatechin 3-gallate (EGCG) in LPS-activated BV-2 microglia cells. *Brain Sci* 13:632
62. Cui H, Xu Z, Qu C (2020) Tetramethylpyrazine ameliorates isoflurane-induced cognitive dysfunction by inhibiting neuroinflammation via miR-150 in rats. *Exp Ther Med* 20:3878–3887
63. Song YY, Yuan Y, Shi X, Che YY (2020) Improved drug delivery and anti-tumor efficacy of combinatorial liposomal formulation of genistein and plumbagin by targeting Glut1 and Akt3 proteins in mice bearing prostate tumor. *Colloids Surf B Biointerfaces* 190:110966
64. Finlay CM, Parkinson JE, Zhang L, Chan BHK, Ajendra J, Chenery A, Morrison A, Kaymak I, Houlder EL, Murtuza Baker S, Dickie BR, Boon L, Konkel JE, Hepworth MR, MacDonald AS, Randolph GJ, Rückerl D, Allen JE (2023) T helper 2 cells control monocyte to tissue-resident macrophage differentiation during nematode infection of the pleural cavity. *Immunity* 56:1064–1081
65. Dias BT, Dias-Teixeira KL, Godinho JP, Faria MS, Calegari-Silva T, Mukhtar MM, Lopes U, Mottram JC, Lima A (2019) Neutrophil elastase promotes *Leishmania donovani* infection via interferon-β. *FASEB J* 33:10794–10807
66. Yan C, Wu J, Xu N, Li J, Zhou QY, Yang HM, Cheng XD, Liu JX, Dong X, Koda S, Zhang BB, Yu Q, Chen JX, Tang RX, Zheng KY (2020) TLR4 deficiency exacerbates biliary injuries and peribiliary fibrosis caused by *Clonorchis sinensis* in a resistant mouse strain. *Front Cell Infect Microbiol* 10:526997
67. Schick J, Altunay M, Lacorcia M, Marschner N, Westermann S, Schluckebier J, Schubart C, Bodendorfer B, Christensen D, Alexander C, Wirtz S, Voehringer D, da Costa CP, Lang R (2023) IL-4 and helminth infection downregulate MINCLE-dependent macrophage response to mycobacteria and Th17 adjuvanticity. *Elife* 12:e72923
68. Paradise WA, Vesper BJ, Goel A, Waltonen JD, Altman KW, Haines GK, Radosevich JA (2010) Nitric oxide: perspectives and emerging studies of a well known cytotoxin. *Int J Mol Sci* 11:2715–2745
69. Moghimi SM, Hunter AC, Murray JC (2001) Long-circulating and target-specific nanoparticles: theory to practice. *Pharmacol Rev* 53:283–318

Publisher's Note

Springer Nature remains neutral with regard to jurisdictional claims in published maps and institutional affiliations.